Effect of Materials Positioning on Dissimilar Modified Friction Stir Clinching between Aluminum 5754-O and 2024-T3 Sheets

Zhou Haiyan[1,*] and Kush P. Mehta[2,3,#]
[1] *Wenzhou Business College, Zhejiang Wenzhou, China*
[2]*Advanced Manufacturing and Materials research group, Department of Mechanical Engineering, School of Engineering, Aalto University, Espoo, Finland*
[3] *Department of Mechanical Engineering, School of Technology, Pandit Deendayal Petroleum University, Raisan, Gandhinagar, India*

[#]Corresponding author: Kush_2312@yahoo.com,
*Co-Corresponding author: zengr75@126.com

Abstract

Dissimilar welding in lap joint configuration between AA5754-O and AA2024-T3 materials is successfully performed using novel technique of Modified Friction Stir Clinching (MFSC) process, wherein materials positioning is analyzed in this investigation. The results revealed that materials positioning in dissimilar MFSC between AA2024-T3 and AA5754-O greatly influences joint properties and grain formation behavior in size, shape and orientations. The superior protuberance leveling of keyhole without any defects and with highest fracture load of 1483 N having fascinating mixing features between AA5754-O and AA2024-T3 were obtained when AA2024-T3 material was kept on top of AA5754-O during second phase of MFSC. Dominated ductile fracture characterized as intergranular fracture mode with secondary cracks and quasi cleavage dimples were also observed in both MFSC.

Keywords: Keyhole; Dissimilar welding; Microstructure; Modified Friction Stir Clinching; Properties.

1. Introduction

As a solid-state process, friction-based joining is considered as one of the most promising techniques to obtain excellent welds in similar and dissimilar materials that leads number of advantages over fusion and resistance-based processes [1-5]. Developments in Friction Stir Welding (FSW), Friction Stir Spot Welding (FSSW), and Friction Stir Clinching have attained popularity in lap joint configurations, wherein the formation of keyhole is inevitable and considered as one of the undesirable issues concerning active location of stress

concentration and corrosion [3,6]. However, to eliminate/repair this keyhole (exit-hole), different techniques such as modified friction stir clinching (MFSC) [7,8], exit-hole repair with probe less tools [9, 10], refill FSSW [11], and application of consumable bit [12] are evolved as recent progress that subsequently increases the acceptability of these processes in different industrial sectors. Different materials are welded with these processes, wherein majority of the investigations are carried out on aluminum alloys (AA) considering excellent weldability in solid state phase. Dissimilar welds are extensively applied to structural components of transport industries based on weight and cost reduction capabilities with increased mechanical performances. Welding of different combinations such as AA7075 to AA2024, AA7075 to AA2198, AA6022 to AA5182, AA6061 to AA5052, AA2024 to AA6061, and AA5754 to AA2024 are developed and analyzed with aforementioned friction-based joining, wherein the combination of AA5754 to AA2024 is reported limited [11-15]. The differences in chemical compositions, physical and mechanical properties of these two alloys are large that subsequently leads challenges in welding. Available literature of AA5754 to AA2024 FSSW are focused on optimization of process parameters to obtain better joint properties [14–17]. Investigations on materials mixing and process-properties correlations for AA5754 to AA2024 combination of joints are lacking. On the other hand, recent development of MFSC is only investigated for dissimilar combination of AA2024 to AA7075. Secondary operation of probe-less tool is subjected to compress the friction stir clinched material from the reversing side that in turn leads to the advantages of protuberance keyhole leveling with exciting features of material mixing over conventional friction-based joining [6,7,18,19]. Considering a knowledge gap for the topic of AA5754 to AA2024 MFSC, it is meaningful to establish the materials mixing features and mechanical properties of this dissimilar joints under the effect of materials positioning in lap joint configuration. Therefore, in this investigation, the differences of intriguing material mixing features and

joint properties are presented for AA5754 to AA2024 MFSC under the effect of material positioning for the first time.

2. Experimental procedure

Lap joint configuration of dissimilar materials of AA2024-T3 and AA5754-O having thickness of 1.6 mm and 1.5 mm respectively were subjected to MFSC. The processing of this dissimilar combination was analyzed under the effect of material positioning with two different conditions. MFSC was performed with its two known phases. In first phase, tool 1 consists of probe was plunged into the workpiece as shown in Fig: 1 (a) and (c). In second phase, tool 2 of probe-less design was plunged from the revert side to eliminate the keyhole with protuberance leveling action as shown in Fig: 1 (b) and (d). The materials position was considered as investigated parameter for present study. Table: 1 represents materials positions considered in this study.

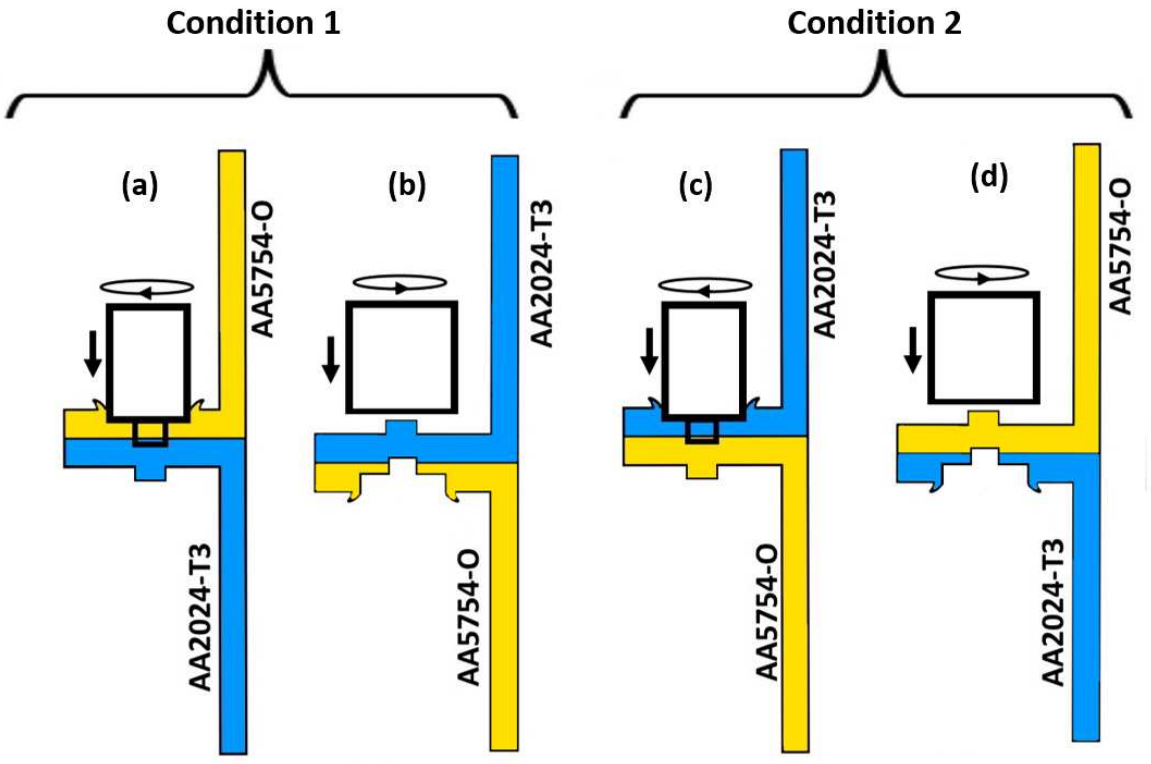

Fig: 1 Processing conditions of workpiece materials positioning performed by MFSC.

Table: 1 Processing condition presentation of workpiece materials positioning in two different phases of MFSC

Processing condition	Phase 1 performed by probe consisted tool	Phase 2 performed by probe-less tool
Condition 1	AA5754-O material was kept on top of AA2024-T3 material	AA2024-T3 material was kept on top of AA5754-O material
Condition 2	AA2024-T3 material was kept on top of AA5754-O material	AA5754-O material was kept on top of AA2024-T3 material

MFSC processing was applied with its two steps using H13 tool material of two different tool designs such as probe consisted tool and probe-less tool (see Fig. 1). Tool 1 was designed with shoulder diameter of 10 mm, cylindrically featured probe diameter of 4 mm and probe length of 2.4 mm, which was used to perform first phase of MFSC. Tool 2 consisted prob-less design with shoulder diameter of 14 mm was applied in the second phase of MFSC with reversing side of first phase. The processing parameters can be pointed out as rotational speed, shoulder plunge depth and dwell time that were kept as 900 rpm, 0.3 mm and 8 seconds respectively during first step. The second step was performed with same parameters of rotational speed and dwell time as kept in first step, whereas shoulder plunge depth was kept as 0.4 mm to obtain protuberance leveling as mentioned in [6,7]. The surface appearance of processed samples is shown in Fig: 2 (a) and (b) for condition 1 and condition 2 respectively.

Material mixing and microstructural features were evaluated using CK45 optical microscopy and electron backscatter diffraction (EBSD). Electro-carved with Barker's reagent by 5 ml HBF_4 in 200 ml water in 25 V for 120 s was applied as a metallographic procedure. The performance of joints was also assessed by load-extension analysis of peel test (Figs: 2c and d) using INSTRON 5500R at a displacement rate of 3 mm/min along with VEGA TESCAN scanning electron microscopy (SEM) of fracture surfaces. Fig: 2 (e) and (f) shows

microstructure of as received base material for AA5754-O and AA2024-T3 respectively, wherein the grains are observed in the direction of rolling.

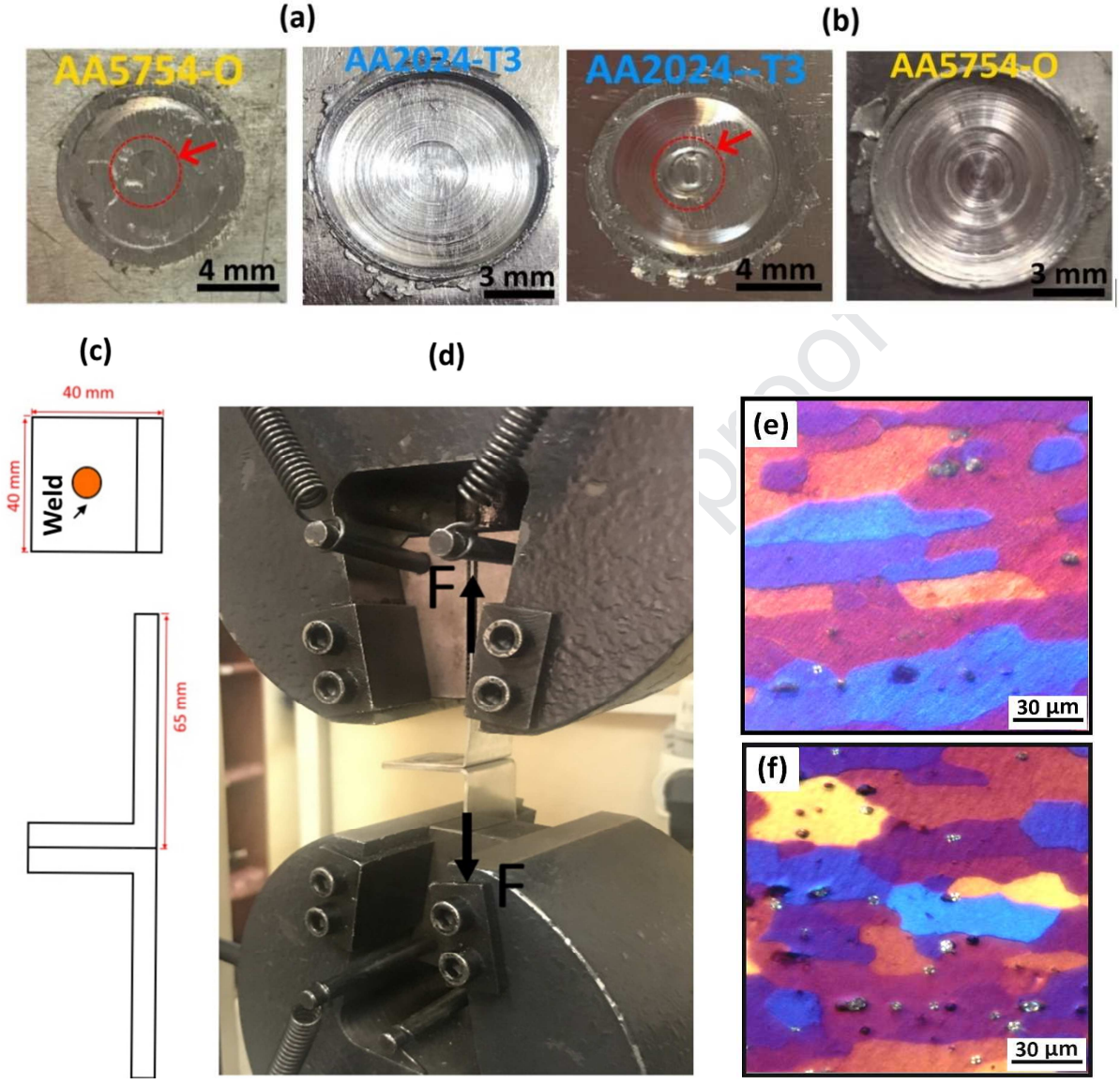

Fig. 2. (a) Surface appearance of condition 1 and (b) Surface appearance of condition 2, (c) Dimensions of peel test, (d) Peel test performance, (e) microstructure of AA5754-O and (f) microstructure of 2024-T3.

3. Results and discussions

The features of materials mixing of AA2024-T3 and AA5754-O after MFSC can be seen from Fig. 3. As obvious, the keyhole is successfully filled in both the cases with intriguing materials mixing features without any defects (see Figs. 3 (a) and (b)). Superior protuberance

leveling was obtained in condition 1 spot weld (Fig. 3 (a)) as compare to other condition 2 spot weld (Fig. 3 (b)). Small void was observed as shown by triangle and arrow in the weld zone of condition 2 weld. Excellent softening of AA5754-O can be obtained compare to AA2024-T3 that in turn helps to fill the cavity of exit-hole due to great visco-plastic flowability when subjected to stirring actions from AA5754-O side and compressive action from AA2024-T3 side of condition 1 weld. Similar materials flow characteristics of AA5754-O was observed in form of hook formation against AA2024-T3 during FSSW when stirred from AA5754-O side [16]. Besides, the high strength and hardness of AA2024-T3 restrict material movements of AA5754-O. Therefore, the consolidation of these two materials can be effectively obtained when AA5754-O is forged by AA2024-T3 during second phase of MFSC with probe-less tool. On contrarily, in case of condition 2, AA2024-T3 material deforms with sharp edge towards direction of tool penetration during first phase with probe consisted tool. This sharp edged material of AA2024-T3 penetrates into AA5754-O material during second phase of MFSC with probe-less tool due to more ductile behavior of AA5754-O compare to AA2024-T3, wherein AA5754-O material was compressed on AA2024-T3. Therefore, a hook like effects were observed due to penetration of AA2024-T3 into AA5754-O in case of Fig. 3 (b) (shown in rectangle), whereas no such features were noticed in Fig. 3 (a). Similar type of hook effect of AA7075 penetration into AA2024 was observed in MFSC between AA7075 and AA2024 [7]. Inadequate material flow in weld of condition 2 was responsible for small void formation in stir zone. Moreover, the shoulder induced unfilled zones (shown by circle and arrow) in Figs. 3 (a) and (b) were observed more in case of condition 2 weld compare to condition 1 weld due to variations in materials flow in both phases of MFSC. Restricted material flow was responsible for inaccurate protuberance leveling as observed in Fig. 3 (b) compared to Fig. 3 (a) with large unfilled zones when subjected with similar compressive and heating actions. Fig. 3 (c)-(e) depicts variations in

grain formation in stir zone and thermo mechanically affected zone (TMAZ) with EBSD for the sample of MFSC of Fig. 3 (a) (i.e. condition 1). Distinct variations in grain formation across these zones can be again correlated with aforementioned discussions. Combined effects of stirring-mixing (during first phase) and forging-consolidation (during second phase) have resulted in fine grains in stir zone compare to TMAZ.

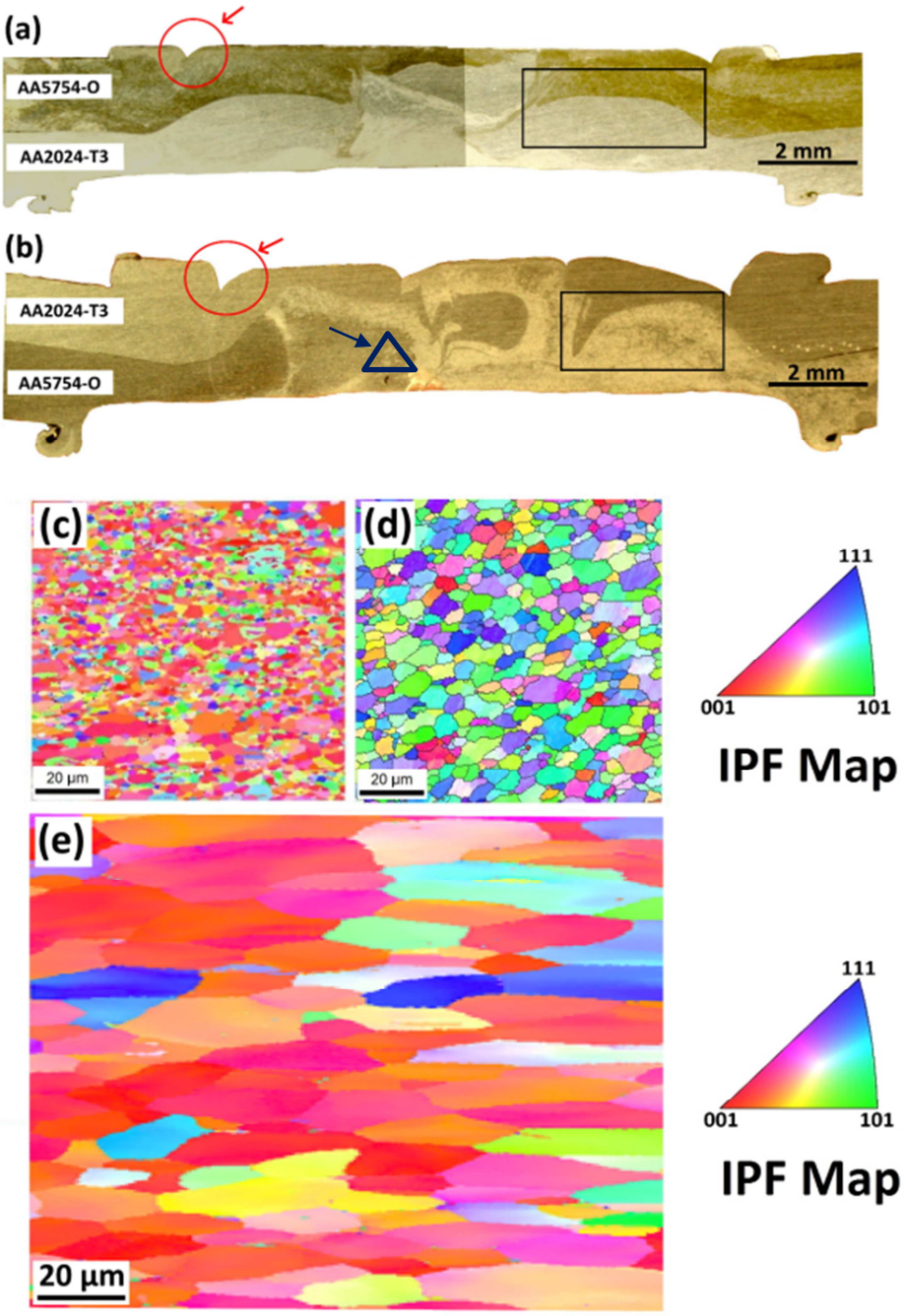

Fig. 3. Macrostructure of (a) condition 1, and (b) condition 2, and EBSD images of condition 1 (c) Stir zone (2024 side), (d) Stir zone (5754 side) and (e) TMAZ (2024 side).

The TMAZ was noticed with large elongated grains (Fig. 3 (e)) distributed in the direction of mechanical deformation caused by forging after stirring actions in contrast to base material that were elongated in the rolling direction (refer Fig. 2 (e) and (f)). Uniform equiaxed grains with clear grain boundaries were noticed in stir zone at AA5754-O (Fig. 3 (d)). Nevertheless, the welds represent a strong heterogeneity in the materials mixing region due to two distinct processing of stirring and forging. The materials mixing region was composed of many small other regions with different microstructure. Some of these regions were composed only of AA2024-T3 while some regions were composed only of AA5754-O and some other regions were composed of both of these alloys. Significantly heterogeneous mixing of AA5754-O and AA2024-T3 materials was observed in case of condition 2 from macrostructure of Fig. 3 (b) compare to condition 1 of Fig. 3 (a). In some region towards AA5754-O side within the stir zone of condition 1, the grains were found larger in size (majorly with orientation of [101]) compared to the one with stir zone of AA2024-T3 (Fig. 3c) (majorly with orientation of [001]) due to local softening experienced in that region experienced by AA5754-O compared to AA2024-T3.

Fig. 4 (a) and (b) show materials flow representation in cross sectional view for condition 1 and condition 2 respectively, when the second phase of MFSC with probe-less tool was performed. It can be represented that the material swirling in combination with forging actions were distributed in different regions of top, bottom, shoulder surface corners and center regions. The flash generated near to the shoulder corner was due to outer materials flow and subsequently resulted in shoulder induced unfilled zones. The materials surrounded by keyhole below the shoulder surface were also moving to outer side from the keyhole periphery as shown in both the cases. However, these materials help to fill the cavity of keyhole as the consolidation of these materials was happened within the same region below shoulder surface due to restriction caused by other non-deformed materials that consequently

flowed inside of keyhole cavity. The material flow in the center region was distinct for condition 1 (Fig. 4 (a)) and condition 2 (Fig. 4 (b)). In case of condition 1, the ductile behavior of AA5754-O that was at bottom side helps in downward materials movement of AA2024-T3 with shoulder forging action and subsequently resulted in enhanced swirling action to fill the keyhole cavity with better solid state diffusion. Besides, AA2024-T3 was having high strength and high hardness compare to AA5754-O that in turn resulted in restriction of materials movement of AA5754-O from the bottom side as shown in Fig: 4 (b). Therefore, the ductile behavior of AA5754-O was resulted in penetration of AA2024-T3 into AA5754-O at the time of forging caused by second phase of MFSC.

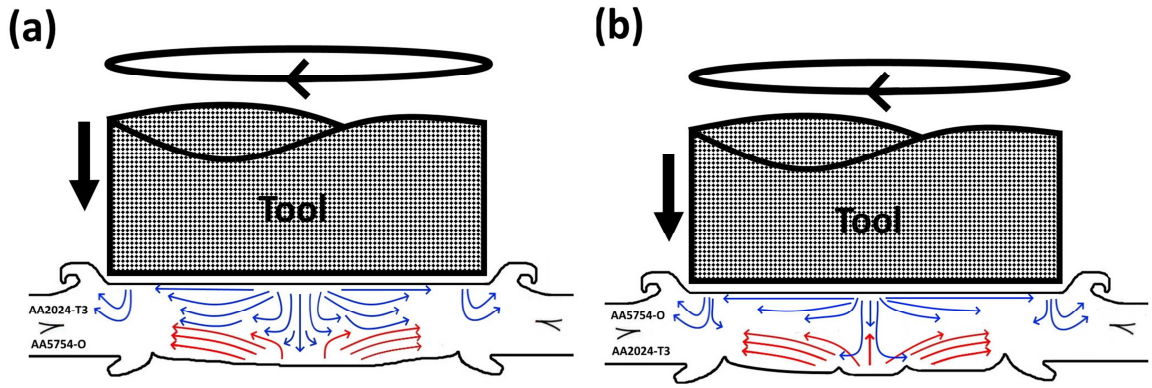

Fig. 4. The schematic of materials mixing during second phase of MFSC (a) condition1 and (b) condition 2.

Fig. 5 indicates intermixing and materials flow after MFSC under the effect of material positioning of AA2024-T3 and AA5754-O. Fig. 5 shows excellent intermixing of both the materials with aforementioned grain size differences and heterogeneity in the same. Materials flow patterns also show interlocking phenomenon with shear bands caused due to mechanical stirring effects and disparity in flow stresses of AA2024-T3 and AA5754-O materials. It can be confirmed that the welds were consisted with a strong heterogeneity in the materials mixing within the weld region. Also, the evidence on many small other regions with different microstructures within the weld zone was provided with Fig. 5 in support of above

macrostructure-EBSD results and discussion. It can be confirmed that some of these regions were composed only of AA2024-T3 while some regions were composed only of AA5754-O and some other regions were composed of both of these alloys along with differences in grain size. These differences are existed owing to distinction in recrystallization behavior between these two materials and/or precipitates dissolving phenomenon of AA2024-T3 material that subsequently caused by workpiece positioning wherein stirring-mixing and forging-consolidation were performed one by one with different materials. Strain hardening and age hardening effects of AA5754 and AA2024 alloys respectively cause differences in these results of grain growth [17] due to experience of strain and thermal effects that are caused two times in two different phases of MFSC such as stirring with probe and forging with probe-less tool. Fig. 5 also shows variations in grain size after experiencing MFSC under the effect of material positioning of AA2024-T3 and AA5754-O. In condition 1, the grain size differences of 5.63 µm (average value of showed region (b)) at AA5754-O and 6.29 µm (average value of showed region (d)) at AA2024-T3 side within the same weld zone were observed. Whereas, in condition 2, the grain size differences of 4.08 µm (average value of showed region (b)) at AA5754-O and 2.86 µm (average value of showed region (d)) at AA2024-T3 side within the same weld zone were observed. In condition 2, AA5754-O was forged on AA2024-T3, wherein more grain refinement may have caused during second phase of MFSC done by probe-less tool due to direct contact of shoulder with ductile material of AA5754-O. Additionally, the stirring was caused in AA2024-T3 during first phase that may have refined AA2024-T3 material with possible precipitates dissolve behavior more significantly. In case of condition 1, the position of workpiece materials was reversed, hence stirring was caused in AA5754-O and forging was applied on AA2024-T3 that in turn resulted with comparatively larger grains than condition 2, however smaller grains in AA5754-O compares to AA2024-T3 within the same zone.

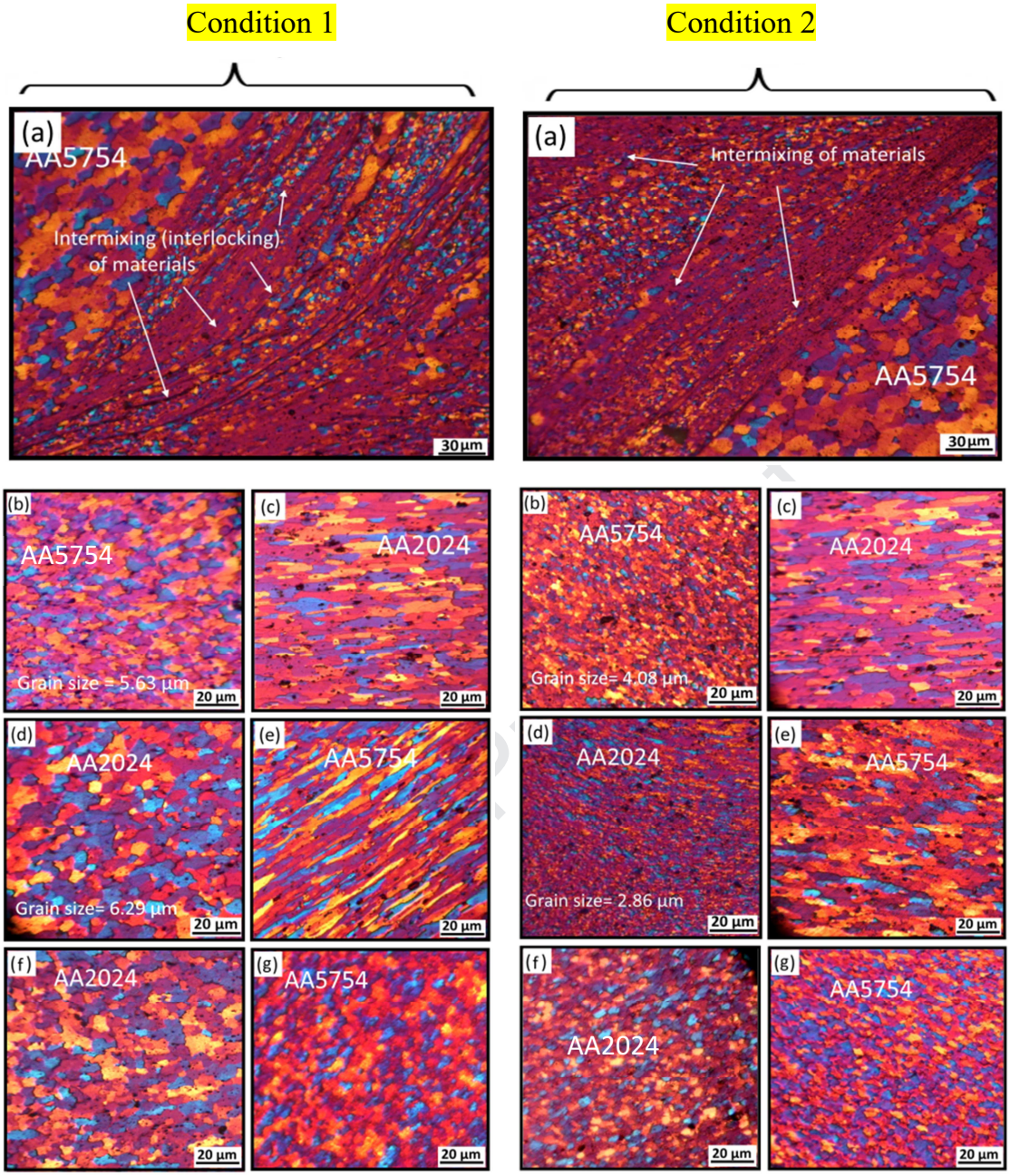

Fig. 5. Microstructure and materials flow within the welds for condition 1 and condition 2.

Fig. 6 shows results of peel tests with load–extension curves and subsequent fractured surfaces of peel tests. The maximum fracture load of 1483 N was noticed for condition 1 weld, whereas the same was 1217 N for condition 2 spot weld. The difference in fracture load and other difference of load-extension curve in terms of smoothness were mainly attributed to defects/no defects, and/or materials behavior after thermo-mechanical processing caused due to materials mixing-consolidation phenomenon. As shown in Fig. 3 (b) for condition 2 spot

weld, the protuberance leveling with second phase of MFSC was improper with void defect in mixed zone. Also, the stirring was performed on AA2024-T3 that is known for second phase particles. It can be possibly observed that the defect subsequently results in fracture propagation point after fracture initiation from shoulder induced unfilled zone during peel test and may have caused disturbances in load-extension curve at 2 mm to 4 mm distance. However, other regions except this defect were observed microscopically sound with better materials mixing and hence large displacement extension can be seen from Fig: 6 (a). Subsequently, it was resulted in lower fracture load compared to the defect free condition 1 spot weld, wherein precipitates of AA2024-T3 may have dissolved during stirring action. It is well known that the precipitates in case of AA2024-T3 material affects mechanical properties variations [20], which were predicted as influenced greatly during stirring-mixing-forging combined actions and subsequently led to uncommon load-extension curve in condition 2. Additionally, the high-density dislocations were identified from transmission electron microscopy as shown in Fig. 6 (b) that was also the large ductility with higher displacement of curve. Fig. 6 (c) shows schematic of fracture path of condition 2 and condition 1 welds, wherein the fracture locations were found similar for both the cases from shoulder impression (i.e. shoulder induced zone) made during the second phase of MFSC. It can be confirmed that the fracture was propagated in the direction of defect from shoulder impression location in case of condition 2 of weld, wherein rapid fall in load value was observed in load-extension curve. Similar fracture propagation in peel test was observed in literature of [21].

Fig. 6 (d)-(i) represents SEM images of fractured surfaces with different magnified locations of fracture. The large dimples were observed in the fractured surfaces of both the cases that in turn indicates ductile fracture mode. The same can be correlated with similar large extension in load-extension curves and high-density dislocations of Fig. 6(b), which shows large elongation caused due to ductile behaviour of obtained joints. The fracture mode can be

further characterized as dominated intergranular fracture mode with secondary cracks and quasi cleavage dimples that are interpreted from Figs. 6 (e), (f), (h) and (i). This fracture mode is in line with fracture of aluminium alloys generally found as ductile fracture [21].

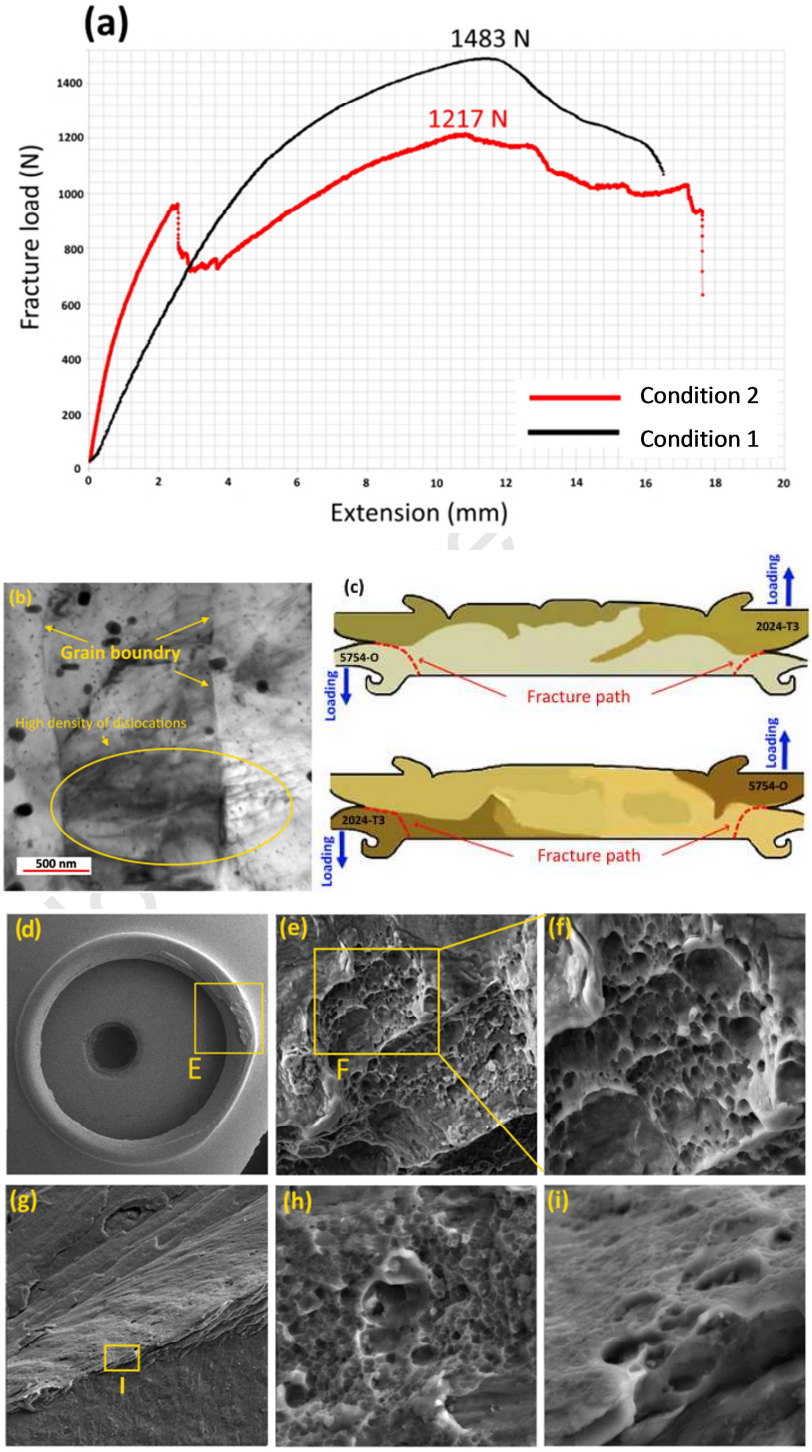

Fig. 6. (a) Load–extension curves of condition 1 and condition 2 welds, (b) Transmission electron microscopic image of condition 2 weld, (c) Schematic of fracture path of condition 2 and condition 1 welds, (d), (e) and (f) SEM of fracture surface of the upper 2024, (g), (h) and (i) 5754.

4. Conclusions

Modified friction stir clinching is successfully established to produced dissimilar lap welding between AA2024-T3 on AA5754-O materials. Effect of materials positioning on materials mixing, microstructure and mechanical properties with peel tests is contrived for dissimilar MFSC. Specific conclusions can be made as follows:

1. Effective materials mixing of stirring bands and interlocking between dissimilar AA2024-T3 on AA5754-O joints can be obtained (with superior protuberance leveling of keyhole) when AA2024-T3 material was kept on top of AA5754-O during second phase of MFSC performed by probe-less tool (i.e. condition 1).
2. Mechanical hooking of AA2024-T3 in AA5754-O, void defect and inadequate protuberance leveling of exit-hole was observed with MFSC performed keeping AA5754-O on AA2024-T3 during second phase of MFSC performed by probe-less tool (i.e. condition 2).
3. Materials positioning in dissimilar MFSC between AA2024-T3 and AA5754-O influences joint properties and materials mixing with distinct grain formation behavior.
4. Highest fracture load of 1483 N was observed when AA2024-T3 material was kept on top of AA5754-O during second phase of MFSC performed by probe-less tool (i.e. condition 1). Dominated ductile fracture characterized as intergranular fracture mode with secondary cracks and quasi cleavage dimples was observed in both MFSC.

References

[1] K. P. Mehta and V. J. Badheka, "A review on dissimilar friction stir welding of copper to aluminum: Process, properties, and variants," *Mater. Manuf. Process.*, 31, 233–254, 2016.

[2] K. P. Mehta, "A review on friction-based joining of dissimilar aluminum – steel joints," *J. Mater. Res.*, 34, 78–96, 2019.

[3] R. S. Mishra and Z. Y. Ma, "Friction stir welding and processing," *Mater. Sci. Eng. R Reports*, 50, 1–78, 2005.

[4] M. Paidar, A. Khodabandeh, H. Najafi and A. Sabour Rouh-aghdamm, "Effects of the tool rotational speed and shoulder penetration depth on mechanical properties and failure modes of friction stir spot welds of aluminum 2024-T3 sheets, " *J. Mech. Sci. Technol.,* 28, 4893-4898, 2014.

[5] K. P. Mehta, P. Carlone, A. Astarita, F. Scherillo, and F. Rubino, "Conventional and cooling assisted friction stir welding of AA6061 and AZ31B alloys," *Mater. Sci. Eng. A*, 759, 252–261, 2019.

[6] P. C. Lin and S. M. Lo, "Friction stir clinching of alclad AA2024-T3 sheets," *Int. J. Adv. Manuf. Technol.*, 92, 2425–2437, 2017.

[7] M. Paidar, S. Ghavamian, O. O. Ojo, A. Khorram, and A. Shahbaz, "Modified friction stir clinching of dissimilar AA2024-T3 to AA7075-T6: Effect of tool rotational speed and penetration depth," *J. Manuf. Process.*, 47, 157–171, 2019.

[8] M. Paidar, O. O. Ojo, A. Moghanian, A. S. Karapuzha, and A. Heidarzadeh, "Modified friction stir clinching with protuberance-keyhole levelling: A process for production of welds with high strength," *J. Manuf. Process.*, 41, 177–187, 2019.

[9] K. P. Mehta, R. Patel, H. Vyas, S. Memon, and P. Vilaça, "Repairing of exit-hole in dissimilar Al-Mg friction stir welding: Process and microstructural pattern," *Manuf. Lett.*, 23, 67–70, 2020.

[10] K. P. Mehta and R. Patel, "On fsw keyhole removal to improve volume defect using pin less tool," *Key Eng. Mater.*, 821 KEM, 215–221, 2019.

[11] Z. Shen *et al.*, "Material flow during refill friction stir spot welded dissimilar Al alloys using a grooved tool," *J. Manuf. Process.*, 49, 260–270, 2020.

[12] Y. X. Huang *et al.*, "New technique of filling friction stir welding," *Sci. Technol. Weld. Join.*, 16, 497–501, 2011.

[13] O. O. Ojo, E. Taban, and E. Kaluc, "Friction stir spot welding of aluminum alloys: A recent review," *Mater. Test.*, 57, 609–627, 2015.

[14] Y. Bozkurt and M. K. Bilici, "Application of Taguchi approach to optimize of FSSW parameters on joint properties of dissimilar AA2024-T3 and AA5754-H22 aluminum alloys," *Mater. Des.*, 51, 513–521, 2013.

[15] Y. Bozkurt and M. K. Bilici, "Taguchi optimization of process parameters in friction stir spot welding of AA5754 and AA2024 alloys," *Adv. Mater. Res.*, 1016, 161–166, 2014.

[16] M. K. Abbass, S. K. Hussein, and A. A. Khudhair, "Optimization of Mechanical Properties of Friction Stir Spot Welded Joints for Dissimilar Aluminum Alloys (AA2024-T3 and AA 5754-H114)," *Arab. J. Sci. Eng.*, 41, 4563–4572, 2016.

[17] Y. Bozkurt, S. Salman, and G. Çam, "Effect of welding parameters on lap shear tensile properties of dissimilar friction stir spot welded aa 5754-h22/2024-t3 joints," *Sci. Technol. Weld. Join.*, 18, 337–345, 2013.

[18] M. Paidar, R. V. Vignesh, A. Khorram, O. O. Ojo, A. Rasoulpouraghdam, and I. Pustokhina, "Dissimilar modified friction stir clinching of AA2024-AA6061 aluminum alloys: Effects of materials positioning," *J. Mater. Res. Technol.*, 2020.

[19] M. Paidar, R. Vaira Vignesh, A. Moharrami, O. O. Ojo, A. Jafari, and S. Sadreddini, "Development and characterization of dissimilar joint between AA2024-T3 and AA6061-T6 by modified friction stir clinching process," *Vacuum*, 176, 109298, 2020.

[20] Y. C. Lin, Y. C. Xia, Y. Q. Jiang, H. M. Zhou, and L. T. Li, “Precipitation hardening of 2024-T3 aluminum alloy during creep aging,” *Mater. Sci. Eng. A*, 565, 420–429, 2013.

[21] Z. Li, Y; Shan, H; Zhang, Y; J. Bi, J; Luo, “Failure Mode of Spot Welds Under Cross - Tension and Coach - Peel Loads,” *Weld. J.*, 96, 2017.

Highlights

- ✓ Dissimilar welding in lap joint configuration between AA5754-O and AA2024-T3 materials is successfully performed using novel technique of Modified Friction Stir Clinching (MFSC) process.

- ✓ Materials positioning in dissimilar MFSC between AA2024-T3 and AA5754-O influences joint properties and grain formation behavior in size, shape and orientations.

- ✓ Highest fracture load of 1483 N was observed in 5754/2024 spot weld.

Conflict of Interest and Authorship Conformation Form

Please check the following as appropriate:

- All authors have participated in (a) conception and design, or analysis and interpretation of the data; (b) drafting the article or revising it critically for important intellectual content; and (c) approval of the final version.
- This manuscript has not been submitted to, nor is under review at, another journal or other publishing venue.
- The authors have no affiliation with any organization with a direct or indirect financial interest in the subject matter discussed in the manuscript
- The following authors have affiliations with organizations with direct or indirect financial interest in the subject matter discussed in the manuscript:

Author's name	Affiliation
Zhou Haiyan	Wenzhou Business College, Zhejiang Wenzhou, China
Kus P Mehta	Department of Mechanical Engineering, School of Technology, Pandit Deendayal Petroleum University, Raisan, Gandhinagar, India